JMEPEG (2012) 21:2173–2176
DOI: 10.1007/s11665-012-0141-3
©ASM International
1059-9495/$19.00

Development of Weld Metal Microstructures in Pulsed Laser Welding of Duplex Stainless Steel

F. Mirakhorli, F. Malek Ghaini, and M.J. Torkamany

(Submitted October 30, 2011)

The microstructure of the weld metal of a duplex stainless steel made with Nd:YAG pulsed laser is investigated at different travel speeds and pulse frequencies. In terms of the solidification pattern, the weld microstructure is shown to be composed of two distinct zones. The presence of two competing heat transfer channels to the relatively cooler base metal and the relatively hotter previous weld spot is proposed to develop two zones. At high overlapping factors, an array of continuous axial grains at the weld centerline is formed. At low overlapping factors, in the zone of higher cooling rate, a higher percentage of ferrite is transformed to austenite. This is shown to be because with extreme cooling rates involved in pulsed laser welding with low overlapping, the ferrite-to-austenite transformation can be limited only to the grain boundaries.

Keywords duplex stainless steel, microstructure, pulsed laser welding, solidification

1. Introduction

Duplex stainless steels (DSS) are widely used in petrochemical and chemical processings because of the combination of corrosion resistance and advantageous mechanical properties. The wrought alloys microstructure at room temperature is composed of austenite and ferrite phases (Ref 1, 2). However, the microstructure resulting from a fusion welding process can be significantly different because of the cooling rates involved (Ref 3-5). Figure 1 depicts a typical DSS alloy that would solidify completely into ferrite and then, while cooling through solid state transformation, it partially transforms into austenite (Ref 1, 2). Considering the comparatively higher cooling rates involved in welding processes, the weld metal and the HAZ microstructure could contain higher amounts of ferrite phase than the base metal. This also can affect the mechanical and corrosion resistance properties of DSS welds (Ref 2-7).

Welding DSS alloys with continuous power laser has been the subject of previous research studies (Ref 8-10). It is shown that the low heat input and consequently high cooling rates can lead to the formation of higher α/γ ratio. On the other hand, pulsed laser can provide further controls on power and heat input. However, there can be questions on how the microstructure of a DSS alloy is affected by the rapid pulsating nature of the heat source, since consecutive melting and solidification of weld spots would occur (Ref 11-13).

F. Mirakhorli and **F. Malek Ghaini**, Department of Materials Engineering, Tarbiat Modares University, Tehran, Iran; and **M.J. Torkamany**, Iranian National Centre for Laser Science and Technology (INLC), PO Box 14665-576, Tehran, Iran. Contact e-mails: mirakhorli.f@gmail.com. farshidmalek@yahoo.com and mjtorkamany@inlc.ir.

In the present study, the focus is on the evaluation of the microstructure in different regions in the weld metal of a DSS and also analyzing the effect of variation in weld travel speed and pulse frequency.

2. Experimental Procedure

Bead-on-plate laser welding was applied on 2-mm-thick commercial SAF 2205 DSS plate. The base metal chemical composition is given in Table 1. Laser welding machine was IQL-10, with a pulsed Nd:YAG laser connected to a computer controlled working table and with a maximum mean laser power of 400 W. The available range for the laser parameters were 1-1000 Hz for pulse frequency, 0-40 J for pulse energy, and 0.2-20 ms for pulse duration.

During laser welding, argon shielding gas with a coaxial nozzle was used to protect the heated surface from oxidation. Work pieces were polished and cleaned with acetone to be prepared for welding. The welded samples were observed in cross sections from three different perpendicular directions (top, transverse, and longitudinal). The etchant was Beraha (0.7 $K_2S_2O_5$ 20 mL HCl in 100 mL solution). The wrought base metal consisted of 55% ferrite and 45% austenite as measured by image analysis, with an average hardness of 280 HV as measured by a 500 g load. After establishing the range of parameters to achieve an acceptable weld appearance, the experiments were carried out with varying travel speeds and pulse frequencies, as shown in Table 2.

Overlap factor f was calculated by the Eq 1 (Ref 12, 13).

$$O_f = \left(1 - \frac{v/f}{D + vT}\right) \times 100 \quad \text{(Eq 1)}$$

where T is the pulse duration, v is the welding speed, f is the laser frequency, and D refers to the laser spot size on the work piece measured as 0.9 ± 0.1 mm.

3. Results and Discussion

Figure 2 shows the top view of welds at a low and high overlapping. As observed from the figure, the weld spots are clearly distinguishable from each other specially at lower overlapping. When the time (or distance) between two pulses increases, high cooling rates can cause the earlier spots to solidify completely before coincident of the next pulse (Ref 11). On the other hand, when the time (or distance) between two pulses decreases, the former spot temperature can still be high enough to the extent that semisolid condition is dominant and the next pulse can raise the temperature to a degree which can almost disappear the fusion line. The solidification pattern of the weld metal was found to vary with the travel speed and/or frequency because of variations of the overlap factor. With a low overlapping factor, as shown in Fig. 2(a), from a solidification pattern point of view, two zones can be identified:

Zone I is the part of the weld metal which is remelted by the next pulse before becoming cooled thoroughly. In this zone, the grains nucleate on the previous spot epitaxially and grow toward the center.

Zone II refers to a single pulse microstructure which is not affected by the next pulse heat and is solidified mainly from the base metal. In this part, the grain boundaries were relatively finer and more jagged.

Between zones I and II, there exists a very narrow band of material which is affected by the heat of the next pulse welding, i.e., the HAZ of zone I in zone II. In Fig. 2(a), this region is marked as 3, and from a solidification pattern point of view, it is a part of zone II. The development of the observed solidification patterns is because in pulse laser welding, when the weld spots are not too close to each other, the previous weld spot is relatively cool when the next pulse strikes, and therefore, effectively two different competing routes exist for the extraction of heat from any point in the molten weld pool. The first route is directly through the side walls (fusion line with the base metal), and the second route is through the previous weld spot (fusion line between consecutive weld spots). The temperature distribution field of the weld pool is affected by both of these two heat sinks. Proximity of any point in the weld pool to each of these two routes of heat extraction is one of the factors determining the dominant cooling route and solidification orientation. The preferential solidification orientation is also affected by the orientation of the grains on which the weld metal grows epitaxially. Zone 1 shown in Fig. 2(a) is mainly cooled through heat transfer to the previous weld spot (and then to the base metal), but zone 2 is cooled through transferring heat from side walls to the base metal. Also, when weld spots overlap each other extensively, zone 2 almost disappears and becomes only limited to a narrow band just next to the two side walls. In such condition (high overlapping), zone 1 solidification pattern dominates most of the weld metal central part, and they can effectively grow on each other epitaxially without being disturbed by zone 1 grains coming in between. Here, the grains in the consecutive zone 1's form a clear preferred orientation, and the axial solidification pattern is formed as shown in Fig. 2(b). The authors have experienced pulsed laser welding of various alloys including carbon steel, aluminum alloys, and titanium. However, it was in the case of DSS that such progress in understanding of the process of weld microstructures development became possible. It would be interesting to study the weld microstructures in other alloys in the light of the knowledge gained. As stated earlier, solidification in zone 2 is dominated by heat extraction to the side walls, but solidification in zone 1 is dominated by heat extraction to the previous weld spot. The larger grain sizes in zone 1 are due to a higher effective preheat temperature of the material the heat of which escapes to i.e., the metal which itself has been molten just a little earlier. However, the sidewalls are expected to have a lower temperature, as a steeper temperature gradient occurs for solidification of zone 2. Thus, the cooling rate in zone 1 is expected to be comparatively lower resulting in a coarser microstructure. Now, our attention turns to the post

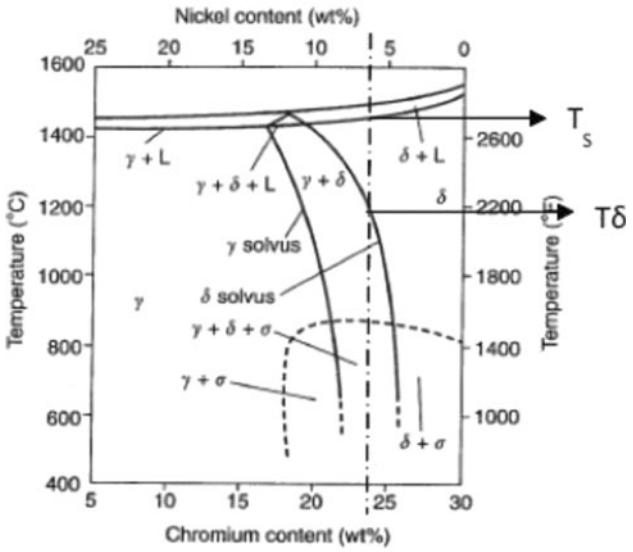

Fig. 1 Pseudo binary section of Fe-Cr-Ni system at 70% iron

Table 2 Weld test conditions

Parameters	Samples A1-A5	Samples B1-B4
Average power, W	110	110, 165, 220, 264
Pulse energy, J	11	11
Pulse duration, ms	6	6
Pulse repetition rate, Hz	10	10, 15, 20, 24
Laser travel speed, mm/s	11.5, 8, 6.67, 4,1.6	6.67
Overlapping factor computed	10.57, 23, 35, 61.5, 83	35%, 55%, 66%, 73%

Table 1 Chemical composition (in wt.%)

Element	C	Si	Mn	P	S	Cr	Ni	Mo	Fe
wt.%	0.03	1.0	1.42	0.023	0.005	22.31	5.48	3.34	Bal.

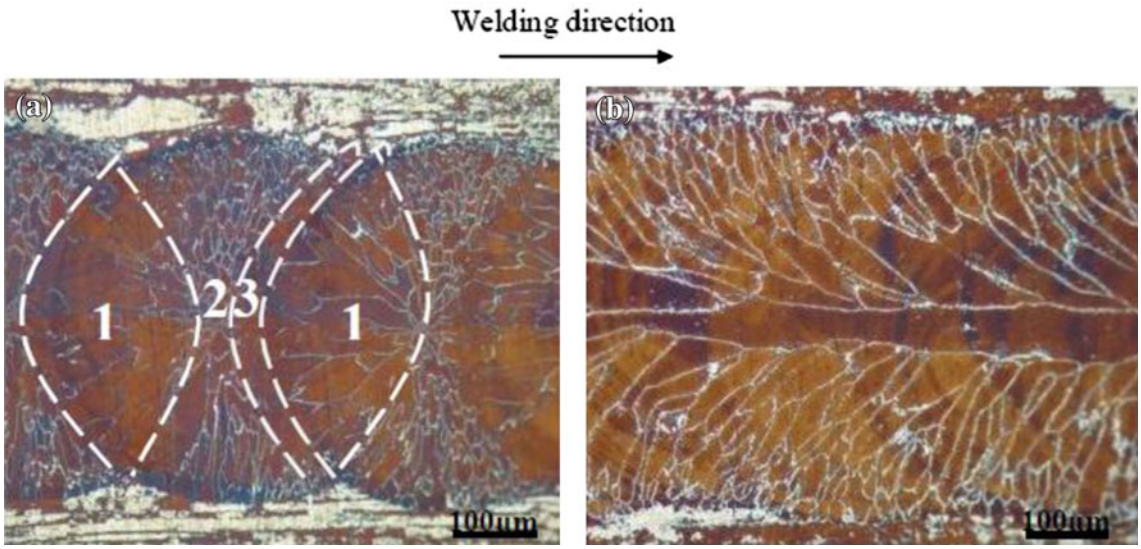

Fig. 2 Microstructures of the welds with various overlap factors as viewed from top direction at (a) 55% (sample B2) and (b) 73% (sample B4)

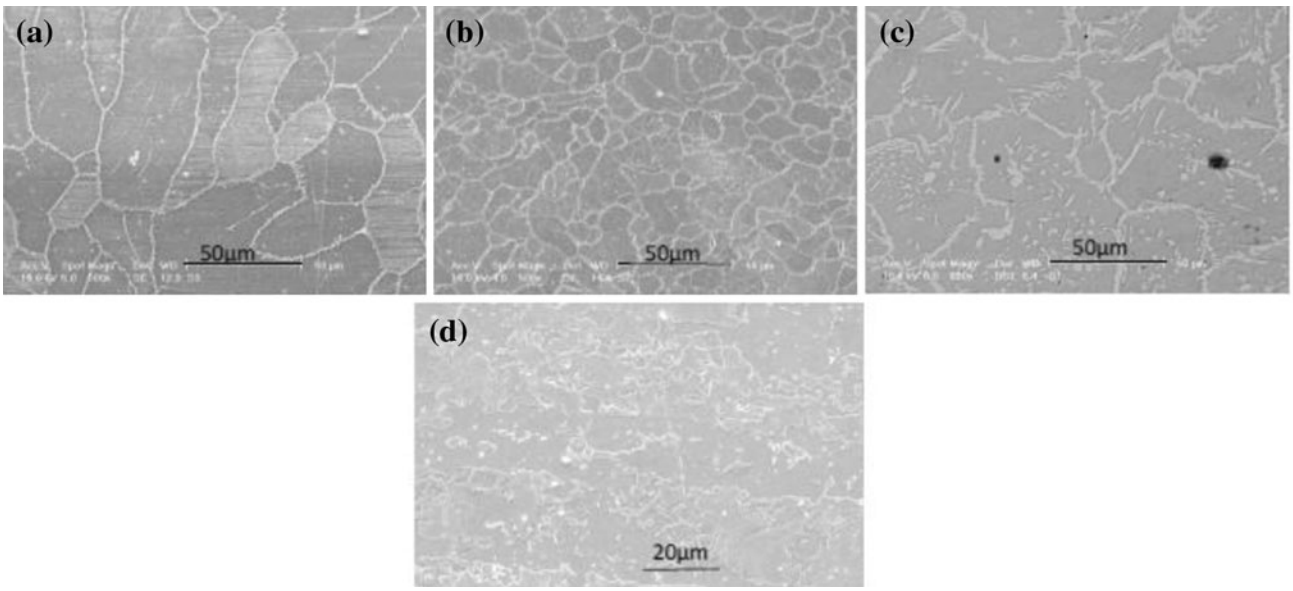

Fig.3 SEM microstructure various parts of the weld metal and the base metal. (a) Zone I in Fig. 2(a). (b) Zone II in Fig. 2(a). (c) The bulk of the weld metal (away from axial grains) in Fig. 2(b). (d) The wrought base metal

solidification transformations and the corresponding microstructural features as shown in Fig. 3. From the phase diagram in Fig. 1, the microstructure of the initial solidifying weld metal is expected to be fully ferritic and austenite, formed during solid state transformations. One might expect to find a higher percentage of austenite in zone 1 because of its lower cooling rate. However, the percentage of austenite in zones 1 and 2 at 55% overlap was measured as 1.6 and 4.8%, respectively. A closer look at Fig. 3(a) and (b) indicates that formation of austenite is limited to the grain boundaries. It seems that at lower overlaps, the cooling rate is so high that formation of austenite has been mainly limited to higher free energy sites at grain boundaries. In this sense, zone 2 material which has a finer solidification structure has provided relatively more preferential sites to form austenite rather than ferrite during the cooling process. However, on increasing the overlap factor to 73%, the cooling rate has decreased so much to form austenite both at the grain boundaries and within the grains, resulting in an austenite content of 18.5%, see Fig. 3(c).

The microhardness in these regions was measured using a 500-g load. At 55% overlap, Zone 1 was found to have a higher hardness of 385 ± 10 HV, in comparison with zone 2 a hardness of 328 ± 10 HV. This lower hardness can be due to the presence of higher amount of austenite in the microstructure of zone 2. The result of Vickers microhardness survey in B4 specimen with a high overlap factor of 73% showed mostly homogenous distribution of microhardness with an average value of 313 HV.

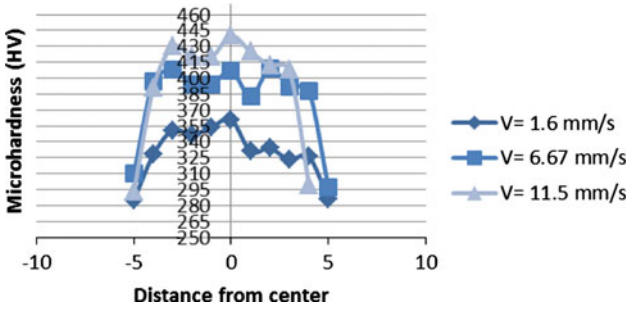

Fig. 4 Microhardness profile along the transverse cross section of the weld in different travel speeds

The microhardness measurement was carried out on a number of transverse cross sections of weld specimens with various overlap factors. The result of hardness surveys is shown in Fig. 4. Basically, the hardness at the center of the weld pool is higher than that of the spots near the fusion line. Higher hardness at the weld center can be due to the higher volume fraction of ferrite phase in this region.

4. Conclusion

The results of pulsed Nd:YAG laser welding DSS are summarized as following:

In pulsed laser welding, an interesting range of microstructures is formed. DSS provided an opportunity to enhance the understanding of how the solidification patterns and the resulting microstructures can develop. When the weld spots do not overlap each other much, two distinct zones of solidification can be identified. One zone is formed under the influence of heat extraction directly to the base metal, while the second one is formed under the influence of heat extraction to the previous weld spot. Proximity to each of these two heat transfer channels and the presence of any strong preferred growth direction of the grains inherited through epitaxial nucleation determines the solidification pattern at any point. At low overlaps, these two zones appear consecutively in the middle part of the weld. By increasing the overlapping, the solidification pattern governed by heat extraction to the previous weld spot can form continuously without disruption leading to an array of axial grains in the middle. The cooling rates involved in pulsed laser welding of DSS can be so high that the formation of austenite from ferrite can be limited to grain boundaries resulting in an observation that some regions with a higher cooling rate may have slightly higher final austenite contents.

References

1. J.C. Lippold and D.J. Kotecki, *Welding Metallurgy and Weldability of Stainless Steels*, Wiley & Sons Inc, New York, 2005
2. Zh.L. Jiang, X.Y. Chen, H. Huang, and X.Y. Liu, Grain Refinement of Cr25Ni5Mo1.5 Duplex Stainless Steel by Heat Treatment, *Mater. Sci. Eng.*, 2003, **A363**, p 263–267
3. H. Sieurin and R. Sandström, Austenite Reformation in the Heat-Affected Zone of Duplex Stainless Steel 2205, *Mater. Sci. Eng.*, 2006, **A418**, p 250–256
4. G. Berglund and P. Wilhelmsson, Fabrication and Practical Experience of Duplex Stainless Steels, *Mater. Des.*, 1989, **10**, p 23–28
5. P. Bala Srinivasan, V. Muthupandi, V. Sivan, P. Bala Srinivasan, and W. Dietzel, Microstructure and Corrosion Behavior of Shielded Metal Arc-Welded Dissimilar Joints Comprising Duplex Stainless Steel and Low Alloy Steel, *J. Mater. Eng. Perform.*, 2004, **15**(6), p 758–764
6. J.D. Kordatos, G. Fourlaris, and G. Papadimitriou, The Effect of Cooling Rate on the Mechanical and Corrosion Properties of SAF2205 (UNS 31803) Duplex Stainless Steel Welds, *Scripta Mater.*, 2001, **44**, p 401–408
7. J.S. Ku, N.J. Ho, and S.C. Tjong, Properties of Electron Beam Welded SAF 2205 Duplex Stainless Steel, *J. Mater. Process. Technol.*, 1997, **63**(1997), p 770–775
8. R.S. Huang, L. Kang, and X. Ma, Microstructure and Phase Composition of a Low-Power YAG Laser-MAG Welded Stainless Steel Joint, *J. Mater. Eng. Perform.*, 2005, **17**(6), p 928–935
9. J. Pekkarinen and V. Kujanpää, The Effects of Laser Welding Parameters on the Microstructure of Ferritic and Duplex Stainless Steels Welds, *Phys. Procedia*, 2010, **5**, p 517–523
10. V. Amigo, V. Bonache, L. Teruel, and A. Vicente, Mechanical Properties of Duple Stainless Steel Laser Joints, *Weld. Int.*, 2006, **20**(5), p 361–366
11. J. Sabbaghzadeh, M.J. Hamedi, F. Malek Ghaini, and M.J. Torkamany, Effect of Process Parameters on Melting Ratio in Overlap Pulsed Laser Welding, *Metall. Mater. Trans.*, 2008, **39B**, p 340–347
12. F. Malek Ghaini, M.J. Hamedi, M.J. Torkamany, and J. Sabbaghzadehb, Weld Metal Microstructural Characteristics in Pulsed Nd:YAG Laser Welding, *Scripta Mater.*, 2007, **56**, p 955–958
13. M.J. Torkamany, M.J. Hamedi, F. Malek, and J. Sabbaghzadeh, The Effect of Process Parameters on Keyhole Welding with a 400 W Nd:YAG Pulsed Laser, *J. Phys.*, 2006, **D39**, p 4563–4567